Available online at www.sciencedirect.com
SCIENCE DIRECT®
Pergamon
Cement and Concrete Research 34 (2004) 849–856
CEMENT AND CONCRETE RESEARCH

Hydration reactions of cement combinations containing vitrified incinerator fly ash

Thomas D. Dyer, Ravindra K. Dhir*

Concrete Technology Unit, Department of Civil Engineering, University of Dundee, Dundee DD1 4HN, UK

Received 28 August 2002; accepted 27 September 2003

Abstract

One treatment option for municipal solid waste incinerator fly ash (IFA) is vitrification. The process yields a material containing reduced levels of trace metals relative to the original ash. The material is glassy and potentially suitable as a cement component in concrete. This paper examines the vitrification of an IFA and studies the hydration reactions of combinations of this vitrified material and Portland cement (PC). Isothermal conduction calorimetry, powder X-ray diffraction (XRD), thermogravimetry (TG) and scanning electron microscopy were employed to study the hydration reactions. As the levels of vitrified ash increase, the quantities of AFt phase produced decrease, whilst quantities of AFm phase increase, due to the reduced levels of sulfate in the vitrified ash. The levels of calcium silicate hydrate (CSH) gel (inferred from estimates of quantities of gel-bound water) remain constant at 28 days regardless of vitrified ash content, indicating that the material is contributing toward the formation of this product.
© 2004 Elsevier Ltd. All rights reserved.

Keywords: Thermal treatment; Hydration products; Compressive strength; Heavy metals; Incinerator fly ash

1. Introduction

One way in which the potential environmental hazards posed by incinerator fly ash (IFA) derived from the combustion of municipal solid waste can be minimised is by vitrification—melting the material and subsequently rapidly cooling it to yield a glassy solid [1]. The process of vitrification removes a significant quantity of toxic trace metals due to the volatilisation of many of the compounds containing such metals [2,3]. These compounds can be collected via filters on condensation and may be processed to extract valuable metal components. The remaining material is converted into an essentially benign solid, which can be safely disposed of.

Given the nonhazardous nature of the remaining solid, alternatives to disposal can be considered, including its use in construction applications. One possible application is as a construction aggregate. However, given the potential risk of alkali-silica reaction in using both natural and synthetic silicate-bearing glassy materials as aggregate [4,5], this approach is not ideal. The composition and glassy nature of the material, however, often means that it is capable of undergoing pozzolanic or latent hydraulic reactions in combination with hydrating Portland cement (PC) [6]. The feasibility of this mode of use has been clearly demonstrated [7].

This paper represents an attempt to better understand these reactions through X-ray diffraction (XRD), thermal analysis, isothermal conduction calorimetry measurements and scanning electron microscopy conducted on pastes containing PC and vitrified IFA (VIFA).

2. Materials and methods

2.1. Materials

The IFA used in the study was selected because its composition made it unsuitable for direct combination with PC due to its retarding influence on cement hydration probably because of its high zinc and lead content [8]. The major oxide analysis of the ash (determined using X-ray fluorescence [XRF] spectrometry) is shown in Table 1 along with that for the PC used. The trace metal content of the ash

* Corresponding author. Tel.: +44-1382-344347; fax: +44-1382-345524.
E-mail address: r.k.dhir@dundee.ac.uk (R.K. Dhir).

0008-8846/$ – see front matter © 2004 Elsevier Ltd. All rights reserved.
doi:10.1016/j.cemconres.2003.09.025

Table 1
Major oxide analysis of the PC, IFA and VIFA used for the study

	PC	IFA	IFA, normalised to 100% (including trace metals)	VIFA
CaO	64.9	15.12	16.51	27.65
Al_2O_3	5.0	10.42	11.38	16.33
SiO_2	21.1	18.81	20.54	40.62
K_2O	0.6	5.31	5.80	1.14
Na_2O	0.3	8.00	8.74	2.15
Fe_2O_3	2.7	2.02	2.21	3.35
MnO	0.1	0.06	0.07	0.13
MgO	1.6	1.23	1.34	3.48
P_2O_5	–	0.77	0.84	1.34
TiO_2	0.2	1.57	1.71	2.93
Cl^-	0.03	7.62	8.32	1.45
SO_3^-	3.3	16.52	18.04	1.19

(also measured using XRF spectrometry) is shown in Table 2, whilst the mineralogies of both the IFA and the PC, estimated from powder XRD traces using Rietveld refinement methods, is shown in Table 3. The term "others" in this table refers largely to amorphous material but may include small quantities of unidentified crystalline minerals. The sum of the major oxide and trace metals analyses for the IFA is notably < 100, and it is probable that the remainder of the material largely comprises water and carbon dioxide (which were not analysed for). For this reason, the major oxide analysis in Table 1 is also shown normalised to 100% (including trace metals) for later comparison with the vitrified material.

2.2. Vitrification

The ash was heated in an alumina crucible in a high temperature furnace to a temperature of 1500 °C at a rate of 10 °C/min. After holding at this temperature for 1 h, the crucible was removed and the molten ash was poured onto a stainless steel surface where it was left to cool. The black, glassy solid was then transferred to a ball mill where it was pulverised. The resulting powder was then passed through a 68 μm sieve.

In parallel with this vitrification process, simultaneous thermogravimetry (TG) and differential thermal analysis (DTA) were carried out on a 10 mg IFA sample in a static air atmosphere up to a temperature of 1200 °C at a rate of 20 °C/min.

Table 2
Trace metal oxide analysis of the IFA and VIFA used for the study

	IFA	VIFA
ZnO	2.48	2.63
PbO	0.91	0.11
Sb_2O_3	0.17	0.32
CuO	0.15	0.04
SnO_2	0.12	0.34
Cr_2O_3	0.08	0.11
BaO	0.07	0.00
SrO	0.05	0.05
NiO	0.03	0.02
ZrO_2	0.03	0.03
CdO	0.02	0.00

Table 3
Mineralogical analysis of the PC and IFA used

Mineral phase	Chemical formula	IFA	PC
Calcite	$CaCO_3$	4.0	–
Anhydrite	$CaSO_4$	12.6	7.1
Halite	NaCl	5.8	–
Sylvite	KCl	3.9	–
Quartz	SiO_2	6.3	–
Melilite	$(Ca,Na)_2(Al,Mg)(Si,Al)_2O_7$	9.0	–
Petalite	$LiAlSiO_4$	1.0	–
Friedel's salt	$Ca_4Al_2O_6Cl_2{\cdot}10H_2O$	1.3	–
Albite	$NaAlSi_3O_8$	4.5	–
C_3A	$Ca_3Al_2O_6$	1.7	6.7
C_4AF	$Ca_4Al_2Fe_2O_{10}$	–	9.3
C_3S	Ca_3SiO_5	–	48.6
C_2S	Ca_2SiO_4	–	24.3
Portlandite	$Ca(OH)_2$	–	1.7
Syngenite	$K_2Ca(SO_4)_2{\cdot}H_2O$	–	2.3
Others	–	49.9	–

2.3. Compressive strength

Compressive strength measurements were made at ages of 2, 7 and 28 days on mortar prisms (dimensions 40 × 40 × 160 mm), prepared and tested in accordance with BS 196 Part 2 [9]. The procedure involves mixing 450 g of the cement components (PC and VIFA) together with 225 g of tap water in a 5 l mixing bowl. CEN standard sand (1345 g) is then added and mixed thoroughly. The mixture is then transferred to three lightly oiled moulds in two layers and compacted with the aid of a vibrating table. After 24 h of being stored in an atmosphere of 20 °C and relative humidity of 95%, the prisms are demoulded, labelled and stored in a water curing tank at a temperature of 20 ± 2 °C until required.

Specimens were prepared containing VIFA at PC replacements of 10%, 20%, 30% and 40% by mass. Control mortar specimens containing no VIFA were also prepared.

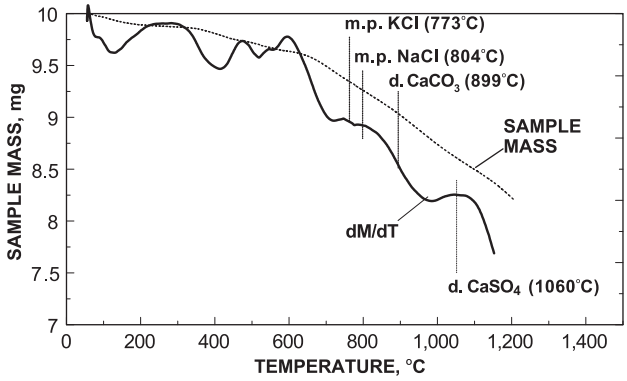

Fig. 1. TG and DTG trace obtained from the IFA. Indicated on the trace are temperatures at which various pure compounds identified in the ash melt or decompose.

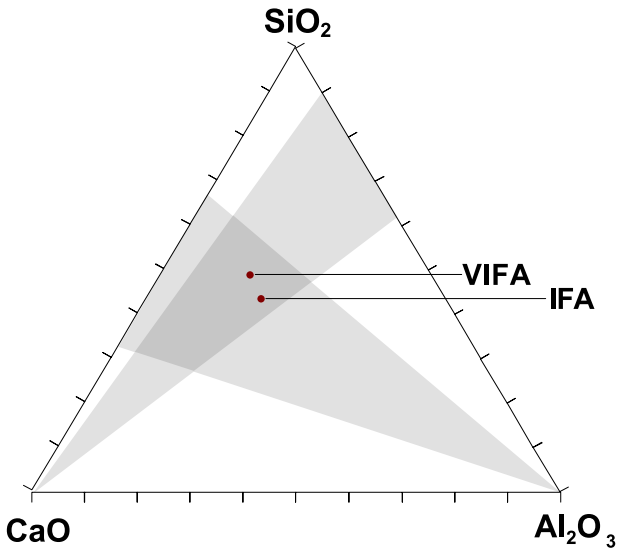

Fig. 2. Position of the original IFA and VIFA on the $CaO\text{-}SiO_2\text{-}Al_2O_3$ ternary diagram. See text for the significance of the shaded areas.

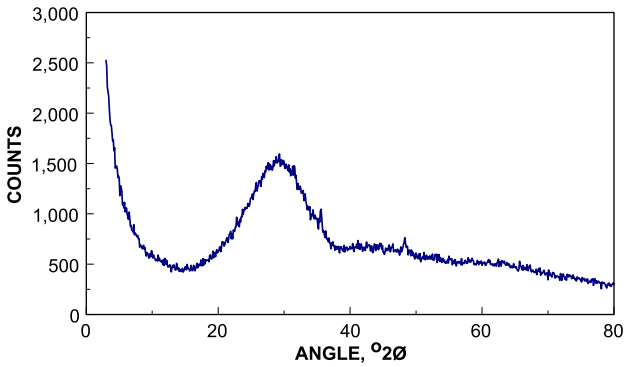

Fig. 3. Powder XRD trace obtained from VIFA.

2.4. Hydration chemistry

A range of methods was used to investigate the hydration chemistry of pastes containing PC and VIFA. The effect of the VIFA on the kinetics of early PC hydration was assessed using isothermal conduction calorimetry. The longer-term reactions occurring in the paste were monitored using TG and powder XRD.

Pastes with a water/cement ratio of 0.5 were used throughout, prepared using distilled water and mixed by hand. Pastes containing 10%, 20% and 40% VIFA by mass were prepared along with controls containing only PC. The pastes used for analysis using TG and XRD were cast into cylindrical polyethylene moulds (internal diameter 25 mm, internal depth 35 mm) and sealed for 24 h. After this period, the lids of the moulds were opened and the specimens were cured in water at a temperature of 20 °C. Specimens were removed at ages of 2, 7 and 28 days and 1 year and hydration was arrested by grinding by hand with acetone before drying under vacuum at a temperature of 40 °C.

2.4.1. Isothermal conduction calorimetry

Thirty grams of solid material were used for the isothermal conduction calorimetry measurements, which were carried out at a temperature of 20 °C. Distilled water was combined with the solids at a water/cement ratio of 0.5. Measurements were carried out for the first 72 h of hydration.

2.4.2. Thermogravimetry

TG measurements were carried out in a nitrogen atmosphere with platinum crucibles containing a 10 mg sample. The furnace temperature was raised from ambient temperature to 1000 °C at a rate of 2 °C/min.

2.4.3. Powder XRD

Powder XRD was carried out using a Philips diffractometer with a Cu$K\alpha$ radiation source and a single crystal

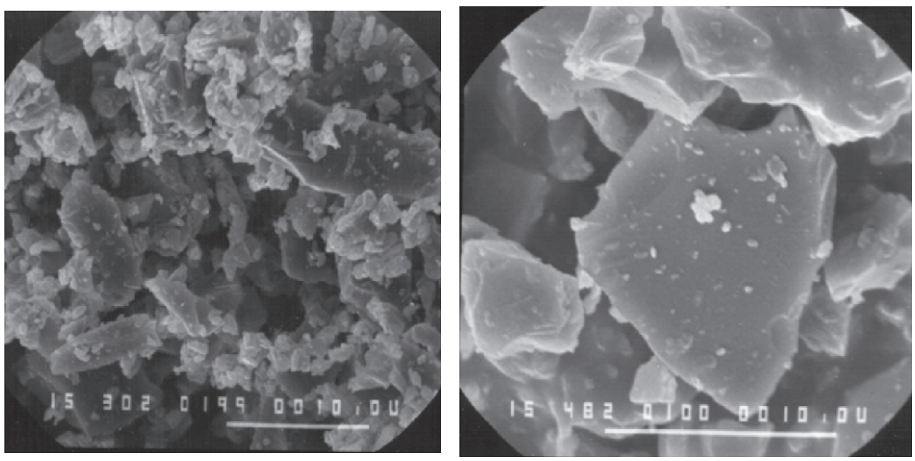

Fig. 4. Scanning electron microscope images of the VIFA after grinding in a laboratory ball mill. The bar on each image corresponds to a distance of 10 μm.

graphite monochromator. An angular range of 3–70° 2θ in 0.05° 2θ increments was used throughout.

Estimates of the quantities of crystalline phases in the pastes were obtained by applying Rietveld refinement techniques to the XRD traces obtained. This was carried out using the computer programmes X-FIT and KOALAR-IET [10–14].

Rietveld refinement is only able to easily handle crystalline phases, and amorphous materials (in this case, in the form of calcium silicate hydrate [CSH] gel and the vitrified ash) cannot be quantified directly. However, by determining the quantity of portlandite ($Ca(OH)_2$) in each paste using TG, this phase could be considered as an internal standard in the pastes. Thus, the quantity of each crystalline phase could be determined from the Rietveld refinement output, and the quantity of total amorphous material was deduced.

2.5. Scanning electron microscopy

Scanning electron microscopy was carried out on a Jeol 35 microscope. Specimens were mounted onto aluminum stubs using double-sided adhesive carbon discs and sputter coated with gold. To ensure that electrical charge was efficiently carried away from cement paste specimen surfaces, a line of silver paint was applied connecting the specimen sides to the stub.

3. Results

3.1. Vitrification

The major oxide analysis of the vitrified ash (obtained using XRF spectrometry) is shown in Table 1. It is apparent that the composition of the resulting glass is enriched in terms of calcium, aluminum, silicon, iron, magnesium, manganese, phosphorous and titanium relative to the original ash. The material contains significantly less sodium and potassium, as well as chloride and sulfate, presumably due to the volatilisation of the chloride- and sulfate-bearing compounds present in the original material.

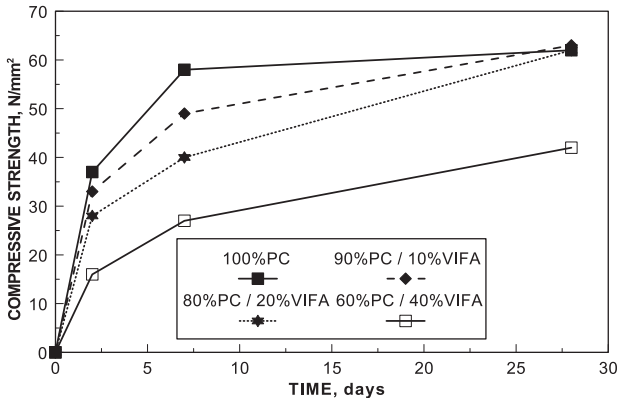

Fig. 5. Compressive strength development of mortars containing VIFA.

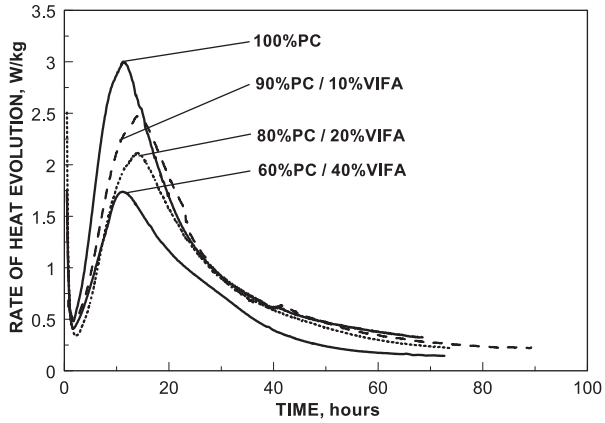

Fig. 6. Rate of heat evolution plots for pastes containing PC and VIFA obtained using isothermal conduction calorimetry.

Fig. 1 shows the TG and differential TG (DTG) traces obtained after heating the ash up to 1200 °C. Clearly, above 600 °C, there is a fairly steady loss of mass due to the volatilisation of various components of the ash. Based on the change in chemical composition of the ash during the vitrification process and the nature of the minerals present, temperatures at which key events occur have been marked on the traces. These events are:

1. The melting of KCl and NaCl that occurs at 773 and 804 °C, respectively [15]. Both compounds tend to volatilise shortly after melting.
2. The thermal decomposition of calcite at around 899 °C to give solid calcium oxide and carbon dioxide gas [16].
3. The thermal decomposition of anhydrite at around 1060 °C [17].

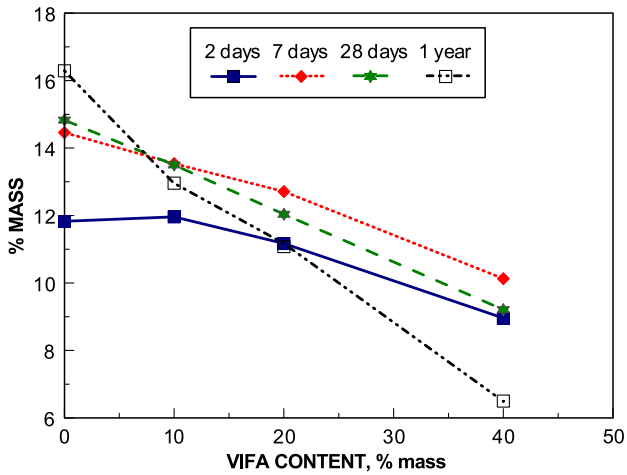

Fig. 7. Levels of portlandite measured in pastes containing PC and VIFA at ages of up to 1 year.

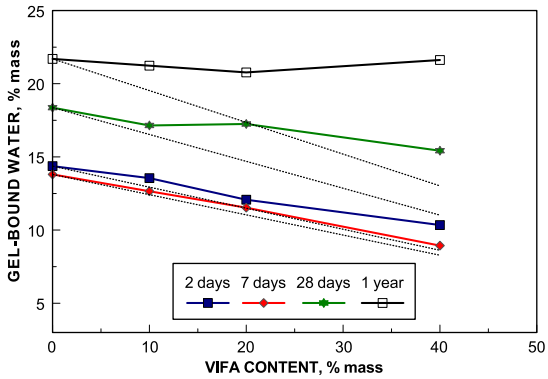

Fig. 8. Estimated levels of gel-bound water measured in pastes containing VIFA at ages of up to 1 year. Dotted lines correspond to gel-bound water levels, which would be expected if the VIFA were entirely inert.

It should be noted that the temperatures at which these events occur are strongly influenced by experimental conditions and the presence of other compounds, so it is unlikely that they occur at these precise temperatures during the vitrification of a complex mixture such as IFA. The relatively close proximity of these temperatures also means that it is difficult to identify individual events, even when the differentiated trace is examined.

Fig. 2 shows the position of both the original IFA and the VIFA on the $CaO\text{-}SiO_2\text{-}Al_2O_3$ ternary diagram. Also shown in this diagram is the region defined by Smolczyk [18] as being inhabited by latent hydraulic materials such as ground granulated blast furnace slags defined by the relationships $0.5 < CaO/SiO_2 < 2.0$ and $0.1 < Al_2O_3/SiO_2 < 0.6$. Clearly, the vitrified ash is positioned well within this region.

Table 2 shows the trace metals analysis of both IFA and VIFA. The VIFA is enriched in terms of zinc, antimony and tin. In contrast, the vitrification process has clearly led to the volatilisation of lead, copper and possibly cadmium and barium, although the low quantities of these two metals make confirmation of their volatilisation difficult.

The powder XRD trace for the vitrified material is shown in Fig. 3. The absence of any sharp diffraction peaks denotes a material that is almost entirely amorphous. Fig. 4 shows particles of VIFA after grinding as observed using the scanning electron microscope. They can be seen to be angular in nature with smooth featureless fracture surfaces similar to ground granulated blast furnace slag.

3.2. Compressive strength development

Fig. 5 shows the development in compressive strength in the mortar prisms containing VIFA along with the control mortar containing only PC as a cement component. With

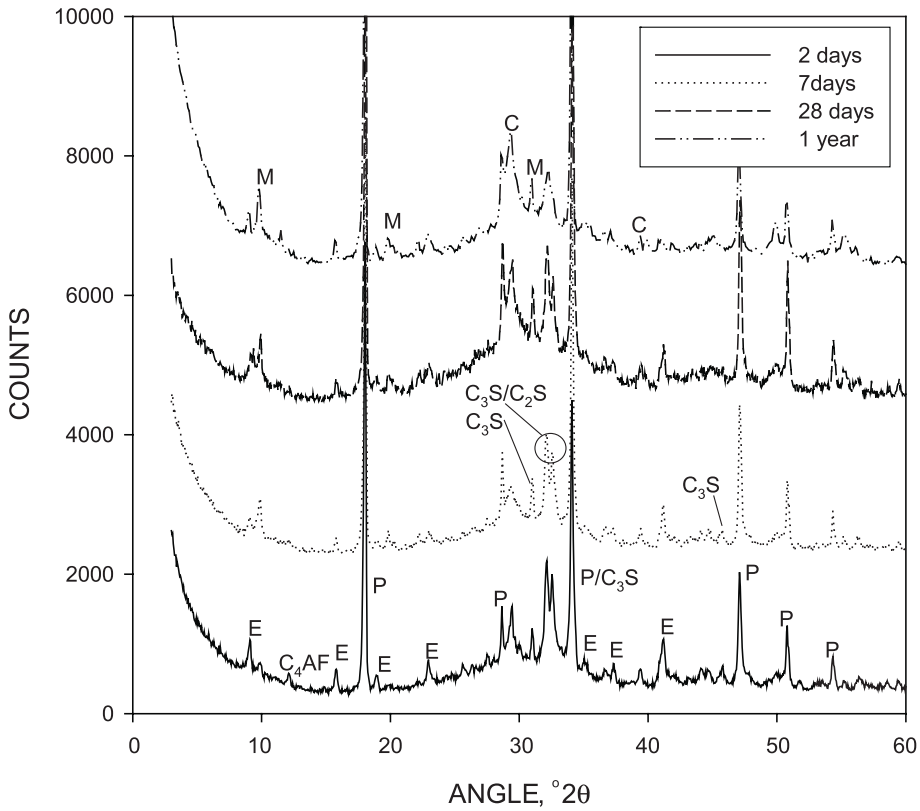

Fig. 9. Powder XRD traces obtained from pastes containing 40% VIFA at ages of 2, 7 and 28 days and 1 year. Traces are offset for clarity. E = ettringite, M = monosulfate, C = calcite, P = portlandite, C_4AF = tetracalcium aluminoferrite, C_2S = dicalcium silicate, C_3S = tricalcium silicate.

relatively low levels of vitrified ash, strengths are initially somewhat lower than the control. However, by 28 days, compressive strengths matching those of the control are achieved. When VIFA makes up a more significant proportion of the cement fraction, strengths lower than the control are achieved even at an age of 28 days.

3.3. Isothermal conduction calorimetry

Fig. 6 shows the isothermal conduction calorimetry curves obtained from the full range of combinations of VIFA and PC. The kinetics of PC hydration are only slightly modified by the presence of the vitrified material, with a slight retarding effect evident in combinations containing 10% and 20% VIFA. It is of interest to note that no retardation of PC hydration is observed for the 40% VIFA paste.

3.4. Thermal analysis and powder XRD

Fig. 7 shows the quantities of portlandite measured in each paste at ages of 2, 7 and 28 days and 1 year using TG. In the pastes containing no VIFA, the levels of portlandite increase with time as the compound is generated by the hydration of the calcium silicates present in PC. At early ages, there is also an increase in portlandite in pastes containing VIFA. However, at later ages, portlandite levels drop, implying the occurrence of a reaction between this compound and the VIFA. This drop in portlandite becomes more pronounced as the quantity of VIFA increases.

The products of the reaction of portlandite with VIFA may be both CSH gel and aluminate hydrates in varying quantities, which can strongly influence strength development and other properties. Obtaining a direct measure of CSH content is effectively impossible using powder XRD and thermal analysis alone because XRD cannot easily distinguish between different amorphous materials (in this case, the gel and the VIFA). However, an estimate of the quantity of gel-bound water is possible by subtracting the water associated with the crystalline hydration products, determined using Rietveld refinement, from the total bound water in the paste, determined using TG.

Estimated gel-bound water contents are shown in Fig. 8. Also plotted on this graph (as dotted lines) are the levels of gel-bound water that would be expected if the VIFA was entirely inert. With the exception of a slight drop in gel-bound water between ages of 2 and 7 days, there is an overall increase in gel-bound water as the pastes age. In all cases, the gel-bound water levels exceed those that would be expected for an entirely inert PC replacement, indicating that CSH gel is being generated as a result of the vitrified material's reaction. The rate of increase in gel-

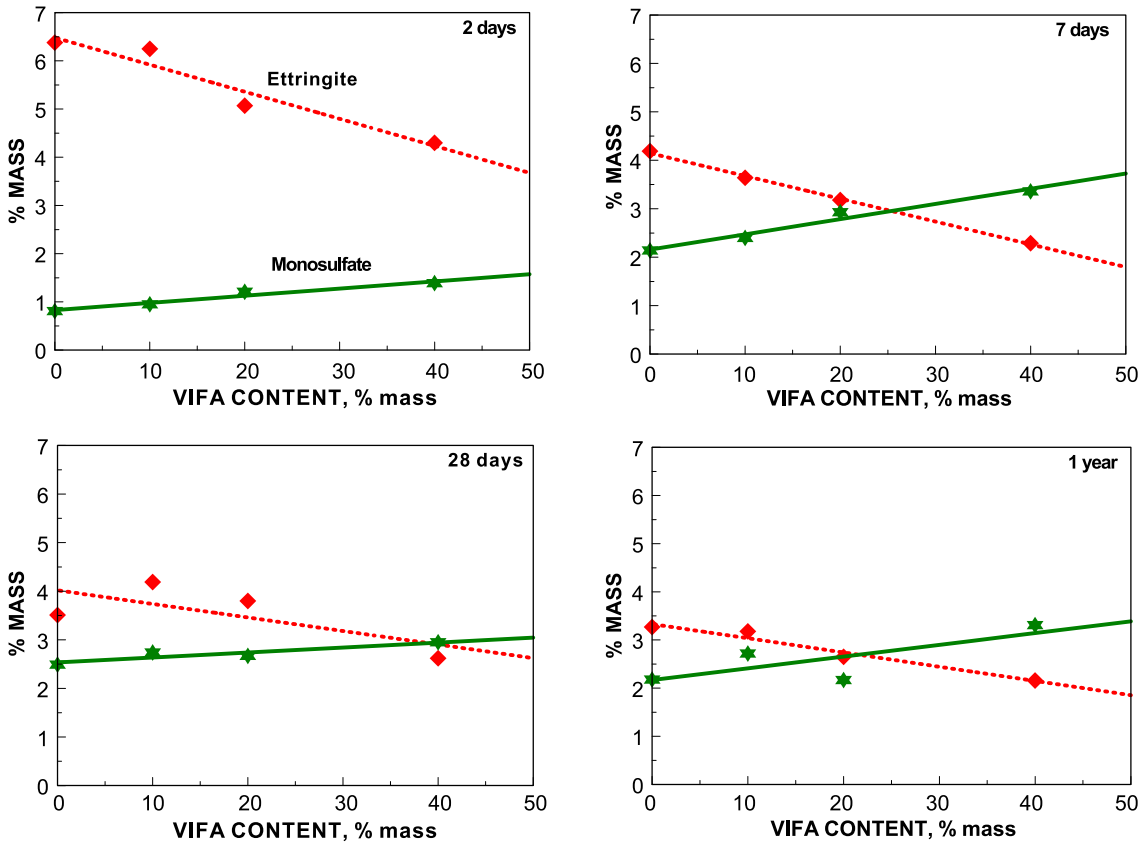

Fig. 10. Ettringite and monosulfate in pastes containing PC and VIFA at ages of up to 1 year.

bound water content rises with VIFA content, so much so that an almost equal quantity is present in all the pastes at an age of 1 year.

Fig. 9 shows diffraction traces obtained from pastes containing 40% VIFA. Two calcium aluminate hydrates were identified in the hydrating pastes—the AFt phase ettringite ($C_6A\hat{S}_3H_{32}$) and the monosulfate AFm phase ($C_4A\hat{S}H_{12}$). The quantities of these two phases in each of the pastes at ages of 2, 7 and 28 days and 1 year are shown in Fig. 10. In all pastes, the formation of these phases follows the pattern normally encountered in hydrating PC. Initially, ettringite is formed in large quantities, but once the soluble sulfates within the paste are exhausted, further reaction of aluminates in both the cement and the vitrified material leads to the conversion of ettringite to monosulfate. There is a general increase in monosulfate content as VIFA levels increase, coupled with a decrease in ettringite levels, due to the relatively low sulfate content of the glassy material. There is a slight increase in the total quantities of AFm and AFt phases as vitrified ash levels increase, indicating that this material is contributing toward their formation.

3.5. Scanning electron microscopy

Fig. 11a–d shows particles of VIFA in the cement matrix at an age of 1 year. The particles show signs of etching presumably resulting from their cementitious reactions. It is worth noting that the particles appear to have been etched more heavily at particular points on their surface, suggesting

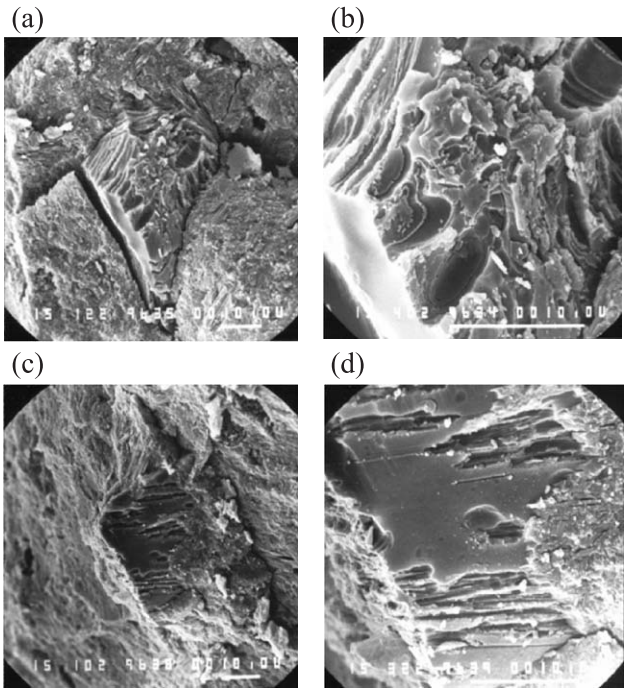

Fig. 11. (a/c) VIFA particles embedded in the cement paste matrix and (b/d) detail of the etched surfaces of these particles.

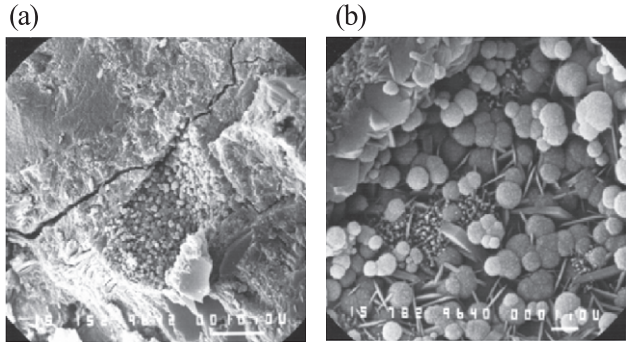

Fig. 12. (a) Impression in the cement paste matrix left by a particle of VIFA and (b) detail of the hydration products at the impression surface.

that the vitrified material's composition varies throughout its volume and may indicate two or more glassy phases.

Fig. 12 shows an impression at the paste fracture surfaces where a particle of VIFA has been pulled out, giving an indication of the nature of the hydration products formed near the surface of these particles, and which are likely to be derived in part from the reactions of the VIFA. CSH gel and hexagonal crystals of either monosulfate or portlandite are clearly visible. However, a significant number of approximately spherical particles can also be seen, whose identity is less certain. Because the only hydration products identified using XRD were ettringite, monosulfate and portlandite, with the remaining hydration products being amorphous, these particles can only be one of the three crystalline hydrate phases, CSH gel or another amorphous phase.

It is most likely that the particles are CSH gel, although their morphology is extremely unusual and may indicate the inclusion of elements other than calcium and silicon.

4. Practical issues

The vitrification and grinding of IFA is clearly a technically feasible option. However, many of the aspects of the process require careful consideration in terms of economic viability (in particular, the high energy demand for melting and grinding) and in terms of environmental issues (the availability of trace metals remaining in the material for leaching).

Because substances volatilised from the ash during vitrification require condensation and collection to prevent release to the environment, one important factor in determining the viability of this process likely is whether some use can be made of this material. In this particular case, the trace metals volatilised from the ash under investigation are of a relatively low value. However, where more valuable components are present in larger quantities, the extraction of these metals from the volatilised fraction may present a means of recouping some of the expense of vitrification.

5. Conclusions

1. Vitrification of fly ash yields a material with lower contents of elements such as sodium, potassium, chlorine, sulfur, lead and copper relative to the original substance. This is the result of volatilisation of these elements at elevated temperatures.
2. The vitrified ash investigated in this study clearly reacts in the presence of PC to form CSH gel. A consequence of this is that the 28-day compressive strengths of mortars containing up to 20% of the vitrified material as a replacement for PC display compressive strengths comparable with mortars containing only PC.
3. The crystalline hydration products formed in pastes containing VIFA are the same as those encountered in pastes containing only PC. There are slightly higher quantities of calcium aluminate hydrates in pastes containing VIFA.
4. Particles of VIFA within the cement matrix show clear signs of reaction. At the surface of the particles, spherical hydration products are visible, the precise nature of which is not clear.

References

[1] R. Kikuchi, Vitrification process for treatment of sewage sludge and incineration ash, Air Waste Manage. 48 (1998) 1112–1115.
[2] A. Jakob, S. Stucki, R.P.W.J. Struis, Complete heavy metal removal from fly ash by heat treatment: influence of chlorides on evaporation rates, Environ. Sci. Technol. 30 (1996) 3275–3283.
[3] S. Stucki, A. Jakob, Thermal treatment of incinerator fly ash: factors influencing the evaporation of $ZnCl_2$, Waste Manage. 17 (1997) 231–236.
[4] C. Polley, S.M. Cramer, R.V. De La Cruz, Potential for using waste glass in Portland cement concrete, J. Mater. Civ. Eng. 10 (1998) 210–211.
[5] S.A. Marfil, P.J. Maiza, Deteriorated pavements due to the alkali-silica reaction. A petrographic study of three cases in Argentina, ASR with glassy aggregates, Cem. Concr. Res. 31 (2001) 1017–1021.
[6] K.-S. Wang, K.-L. Lin, Z.-Q. Huang, Hydraulic activity of municipal solid waste incinerator fly-ash-slag-blended eco-cement, Cem. Concr. Res. 31 (2001) 97–103.
[7] J. Pera, A. Wolde, M. Chababbet, Hydraulic activity of slags obtained by vitrification of wastes, ACI Mater. J., (1996 Nov.–Dec.) 613–618.
[8] C.R. Wilding, A. Walter, D.D. Double, A classification of inorganic and organic admixtures by conduction calorimetry, Cem. Concr. Res. 14 (1984) 185–194.
[9] British Standards Institution, BS EN 196-1, Methods of testing cement: Part 1. Determination of strength, 1995.
[10] H. Berger, Study of the k-alpha emission-spectrum of copper, X-ray Spectrom. 15 (1986) 241–243.
[11] R.W. Cheary, A.A. Coelho, A fundamental parameters approach of X-ray line-profile fitting, J. Appl. Crystallogr. 25 (1992) 109–121.
[12] R.W. Cheary, A.A. Coelho, Synthesising and fitting linear position-sensitive detector step-scanned line profiles, J. Appl. Crystallogr. 27 (1994) 673–681.
[13] D.W. Marquardt, J. Soc. Ind. Appl. Math. 11 (1963) 331–431.
[14] J.C. Nash, Compact Numerical Methods for Computers, Adam Hilger, Bristol, 1990.
[15] G. Aylward, T. Findlay, SI Chemical Data, 3rd ed., Wiley, Chichester, 1994.
[16] T.L. Webb, H. Heystek, The carbonate minerals, in: R.C. Mackenzie (Ed.), The Differential Thermal Investigation of Clays, Mineralogical Society, London, 1957.
[17] J.S. Chinchon, X. Querol, J.L. Fernandezturiel, A. Lopezsoler, Environmental impact of mineral transformations undergone during coal combustion, Environ. Geol. Water Sci. 18 (1991) 11–15.
[18] H.G. Smolczyk, Structure et charactérisation des laitiers, 7th Int. Congr. Chem. Cem., Paris 1 (1980) III-1/3–III-1/17.